EPJ Web of Conferences **66**, 05020 (2014)
DOI: 10.1051/epjconf/ 20146605020


# Antiproton–to–electron mass ratio determined by two-photon laser spectroscopy of antiprotonic helium atoms

A. Sótér[1,a], M. Hori[1], D. Barna[2,3], R. Hayano[2], A. Dax[4], S. Friedreich[5], B. Juhász[5], T. Pask[5], E. Widmann[5], D. Horváth[3], L. Venturelli[6], and N. Zurlo[6]

[1] *Max-Planck-Institut für Quantenoptik, Hans-Kopfermann-Strasse 1, 85748 Garching, Germany*
[2] *Department of Physics, University of Tokyo, Hongo, Bunkyo-ku, Tokyo 113-0033, Japan*
[3] *Wigner Research Center of Physics, H-1525 Budapest, Hungary*
[4] *Paul Scherrer Institut, CH-5232 Villigen, Switzerland*
[5] *Stefan Meyer Institut für Subatomare Physik, Boltzmanngasse 3, Vienna 1090, Austria*
[6] *Dipartimento di Ingegneria dell'Informazione, Università di Brescia and Istituto Nazionale di Fisica Nucleare, Gruppo Collegato di Brescia, I-25133 Brescia, Italy*

**Abstract.** The ASACUSA collaboration of CERN has recently carried out two-photon laser spectroscopy of antiprotonic helium atoms. Three transition frequencies were determined with fractional precisions of 2.3–5 parts in $10^9$. By comparing the results with three-body QED calculations, the antiproton-to-electron mass ratio was determined as 1836.1526736(23).

## 1 Introduction

Antiprotonic helium ($\overline{p}\mathrm{He}^+$) is a three-body atom [1–4] consisting of a helium nucleus, an electron in the 1s state, and an antiproton occupying a Rydberg state with high principal and angular momentum quantum numbers $n \sim \ell + 1 \sim 38$. The transition frequencies of $\overline{p}\mathrm{He}^+$ have been calculated by QED calculations to fractional precisions of $1 \times 10^{-9}$ [5]. The calculations included relativistic and radiative recoil corrections up to order $m_e c^2 \alpha^6 / h$, and nuclear size effects. By comparing the measured and calculated transition frequencies, the antiproton-to-electron mass ratio was determined [4] as 1836.1526736(23).

We have previously measured some $\overline{p}\mathrm{He}^+$ transition frequencies with a fractional precision of $10^{-7} - 10^{-8}$, by single-photon laser spectroscopy [6–9]. The precision was limited by the Doppler broadening of the resonance lines which arose from the thermal motions of the $\overline{p}\mathrm{He}^+$. Recently [4], two-photon transitions of the type $(n, \ell) = (n - 2, \ell - 2)$ [Fig. 1(a)] were excited using two counterpropagating laser beams, such that the Doppler broadening was partially canceled [10].

## 2 Experiment and results

The two-photon transitions were induced between $\overline{p}\mathrm{He}^+$ states with microsecond and nanosecond-scale lifetimes against Auger emission of the electron. After Auger decay, the remaining two-body

[a] e-mail: Anna.Soter@mpq.mpg.de

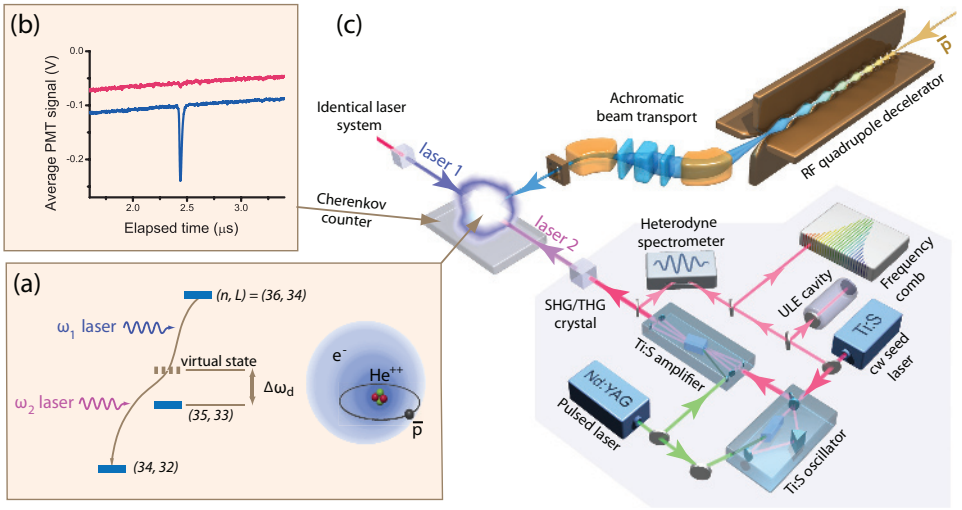


**Figure 1.** Energy level diagram of $\overline{p}^4\mathrm{He}^+$ involved in the two-photon transition $(n, \ell) = (36, 34) \rightarrow (34, 32)$ (a). Cherenkov detector signals for two-photon transition (b). Experimental layout (c). From Ref. [4].

$\overline{p}\mathrm{He}^{2+}$ ion [11] was destroyed by Stark collisions with other helium atoms in the experimental target. The charged pions emerging from the resulting antiproton annihilations were detected by Cherenkov detectors [12] placed around the target. The two-photon resonance condition between the laser and $\overline{p}\mathrm{He}^+$ was revealed as a sharp spike in the rate of antiproton annihilations [Fig. 1 (b)].

Two sets of Ti:Sapphire lasers [13] of pulse length 30-100 ns with a spectral linewidth of $\sim 6$ MHz and a pulse energy of 50–100 mJ were used to excite the antiprotonic transitions. The system included continuous-wave (cw) lasers whose frequencies were measured to a precision of $< 1 \times 10^{-10}$ against a femtosecond optical frequency comb [14].

The experiments were carried out at the Antiproton Decelerator (AD) facility of CERN as part of its atomic physics [15] program. The AD provided 200-ns-long pulsed beams, which contained $\sim 10^7$ antiprotons of kinetic energy 5.3 MeV. The antiprotons were decelerated to $\sim 70$ keV using a radiofrequency quadrupole decelerator [7]. Secondary electron emission detectors measured the spatial profiles of the beam [16]. The $\overline{p}\mathrm{He}^+$ atoms were produced by stopping the antiprotons in a target filled with $^4$He or $^3$He gas at temperature $T \sim 15$ K and pressure $p = 0.8 - 3$ mbar. Two horizontally-polarized laser beams of energy density $\sim 1$ mJ/cm$^2$ fired through the target excited the two-photon transitions.

The Cherenkov signal corresponding to some $10^7$ $\overline{p}\mathrm{He}^+$ atoms is shown in Fig. 1(b), as a function of time elapsed since the arrival of antiproton pulses at the experimental target. Lasers of wavelengths $c/\nu_1 = 417$ and $c/\nu_2 = 372$ nm were tuned to the two-photon transition $(n, \ell) = (36, 34) \rightarrow (34, 32)$, so that the virtual intermediate state lay $\Delta\nu_d \sim 6$ GHz away from the real state $(35, 33)$. This arrangement strongly enhanced the transition probability. The annihilation spike which corresponds to the two-photon transition can be seen at $t = 2.4\mu$s. The intensity of the spike reflects the number of antiprotons populating state $(36, 34)$ [17, 18]. When the 417-nm laser was tuned some $\sim 0.5$ GHz off the two-photon resonance condition, the signal disappeared as indicated in the same figure.

Fig. 2(b) shows the resonance profile measured by detuning the $\nu_1$ laser to $\Delta\nu_d = -6$ GHz, whereas the $\nu_2$ laser was scanned between -1 and 1 GHz around the two-photon resonance defined by $\nu_1 + \nu_2$.

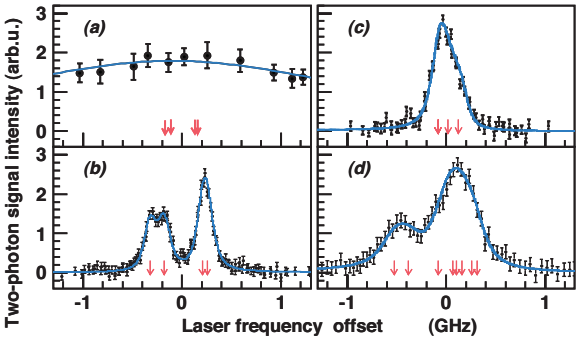


**Figure 2.** Single-photon resonance $(36,34) \rightarrow (35,33)$ of $\overline{p}^4\mathrm{He}^+$ (a). Sub-Doppler two-photon profiles of $(36,34) \rightarrow (34,32)$ (b) and $(33,32) \rightarrow (31,30)$ (c) of $\overline{p}^4\mathrm{He}^+$, and $(35,33) \rightarrow (33,31)$ of $\overline{p}^3\mathrm{He}^+$ (d). Solid lines indicate best fit of theoretical line profiles (see text) and partly overlapping arrows the positions of the hyperfine lines. From Ref. [4].

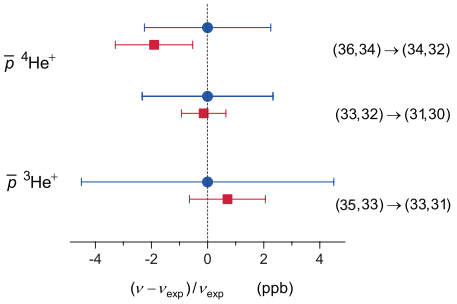


**Figure 3.** Fractional deviation between theoretical (squares) and experimental (circles) transition frequencies of $\overline{p}\mathrm{He}^+$ isotopes measured by two-photon laser spectroscopy. From Ref. [4].

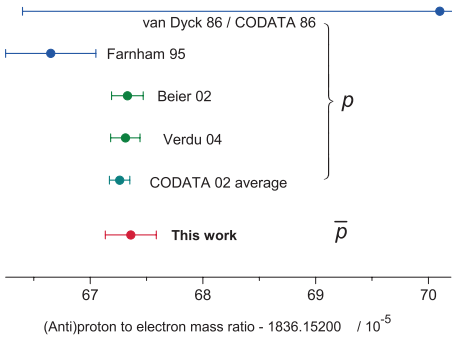


**Figure 4.** Mass ratio $M_{\overline{p}}/m_e$ determined in this work, compared with $M_p/m_e$ measured previously [21–24] and the CODATA 2002 value obtained by averaging them. From Ref. [4].

The linewidth ($\sim$ 200 MHz) of this two-photon resonance is more than an order of magnitude smaller than the Doppler- and power-broadened profile of the single-photon resonance $(36,34) \rightarrow (35,33)$ [Fig. 2(a)]. The two-peak fine structure arises due to the interaction between the electron spin and the orbital angular momentum of the antiproton. We also detected the $(33,32) \rightarrow (31,30)$ and $(35,33) \rightarrow (33,31)$ resonances of $\overline{p}^4\mathrm{He}^+$ and $\overline{p}^3\mathrm{He}^+$, respectively [Fig. 2(c)–(d)]. The latter resonance profile contains eight partially-overlapping hyperfine lines, which arose from the spin-spin interactions of the three constituent particles. The spin-independent transition frequencies $\nu_{\mathrm{exp}}$ were obtained by fitting these measured profiles with a theoretical lineshape (solid lines in Fig. 2) which was determined by numerically solving the rate equations of the two-photon process [10]. The positions of the hyperfine lines were fixed to the theoretical values [19], which have a precision of $< 0.5$ MHz.

The experimental transition frequencies $\nu_{\mathrm{exp}}$ (filled circles with error bars in Fig. 3) agree with the theoretical frequencies $\nu_{\mathrm{th}}$ (squares) within a fractional precision of $(2.3 - 5) \times 10^{-9}$. The calculation

uses the fundamental constants compiled in CODATA2002 [20], such as the $^3$He- and $^4$He-to-electron mass ratios, the Bohr radius, and Rydberg constant. The charge radii of the $^3$He and $^4$He nuclei give relatively small corrections to $\nu_{\rm th}$ of $4-7$ MHz [5]. The correction from the antiproton radius is less than 1 MHz. The theoretical precision of $\nu_{\rm th}$ is now mainly limited by the uncalculated radiative corrections of order $m_e c^2\alpha^8/h$ [5]. When the antiproton-to-electron mass ratio $M_{\overline{p}}/m_e$ in these calculations was increased by a relative amount of $10^{-9}$, the $\nu_{\rm th}$-value changed by 2.3–2.8 MHz. By minimizing the difference between $\nu_{\rm th}$ and $\nu_{\rm exp}$ and considering the systematic errors, we obtained the above antiproton-to-electron mass ratio which yielded the best agreement between theoretical and experimental frequencies. The uncertainty includes the statistical and systematic experimental, and theoretical contributions of $18\times10^{-7}$, $12\times10^{-7}$, and $10\times10^{-7}$. This is in good agreement with previous measurements[21–24] of the proton-to-electron mass ratio (Fig. 4). Under the assumption that CPT invariance is valid (i.e, $M_{\overline{p}} = M_p = 1.00727646677(10)$ u), we derived a value for the electron mass, $m_e = 0.0005485799091(7)$ u [4].

## Acknowledgements

This work was supported by the European Research Council (ERC-StG), European Science Foundation (EURYI), Monbukagakusho (grant no 20002003), Hungarian Research Foundation (K72172), and the Austrian Federal Ministry of Science and Research.

## References

[1] R.S. Hayano, M. Hori, D. Horváth, and E. Widmann, Rep. Prog. Phys. **70**, 1995 (2007).
[2] G.T. Condo, Phys. Lett. **9**, 65 (1964).
[3] J.E. Russel, Phys. Rev. Lett. **23**, 63 (1969).
[4] M. Hori *et al.*, Nature **475**, 484 (2011).
[5] V.I. Korobov, Phys. Rev. A **77**, 042506 (2008).
[6] M. Hori *et al.*, Phys. Rev. Lett. **87**, 093401 (2001).
[7] M. Hori *et al.*, Phys. Rev. Lett. **91**, 123401 (2003).
[8] M. Hori *et al.*, Phys. Rev. Lett. **96**, 243401 (2006).
[9] T. Kobayashi *et al.*, J. Phys. B **46**, 245004 (2013).
[10] M. Hori and V.I. Korobov, Phys. Rev. A **81**, 062508 (2010).
[11] M. Hori *et al.*, Phys. Rev. Lett. **94**, 063401 (2005).
[12] M. Hori *et al.*, Nucl. Instrum. Methods Phys. Res. A **496**, 102 (2003).
[13] M. Hori, and A. Dax, Opt. Lett. **34**, 1273 (2009).
[14] Th. Udem, R. Holzwarth, and T.W. Hänsch, Nature **416**, 233 (2002).
[15] M. Hori and J. Walz, Prog. Part. Nucl. Phys. **72**, 206 (2013).
[16] M. Hori, Rev. Sci. Instrum. **76**, 113303 (2005).
[17] M. Hori *et al.* Phys. Rev. Lett. **89**, 093401 (2002).
[18] M. Hori *et al.* Phys. Rev. A **70**, 012504 (2004).
[19] V.I. Korobov, Phys. Rev. A **73**, 022509 (2006).
[20] P.J. Mohr, B.N. Taylor, Rev. Mod. Phys. **77**, 1–107 (2005).
[21] P.J. Mohr, B.N. Taylor, and D.B. Newell, Rev. Mod. Phys. **80**, 633 (2008).
[22] D.L. Farnham, R.S. Van Dyck Jr., and P.B. Schwinberg, Phys. Rev. Lett. **75**, 3598 (1995).
[23] T. Beier *et al.*, Phys. Rev. Lett. **88**, 011603 (2002).
[24] J. Verdú *et al.*, Phys. Rev. Lett. **92**, 093002 (2004).